Supporting Information

A General Route to Robust Nacre-like Graphene Oxide Films

Zhibing Tan,[†,‡] Miao Zhang,[‡] Chun Li,[,‡] Shiyong Yu[*,†] and Gaoquan Shi[*,‡]*

[†]School of Chemistry and Chemical Engineering, Inner Mongolia University, Hohhot 010021, China.

[‡]Department of Chemistry, Tsinghua University, Beijing 100084, China

* Correspondence should be addressed to: chunli@mail.tsinghua.edu.cn; syyunano@imu.edu.cn; gshi@tsinghua.edu.cn

Table S1. Details on the data of tensile tests.[a]

Sample	Tensile Strength (MPa)	Failure Strain (%)	Toughness (MJ m^{-3})
GO (filtration)	136 ± 21	1.28 ± 0.21	0.88 ± 0.29
GO (evaporation)	115 ± 19	1.33 ± 0.08	0.73 ± 0.14
GO (1% Chitosan)	194 ± 9	3.65 ± 0.60	3.64 ± 0.34
GO (2% Chitosan)	265 ± 10	4.81 ± 0.30	5.93 ± 0.62
GO (4% Chitosan)	254 ± 6	4.85 ± 0.31	6.42 ± 0.25
GO (6% Chitosan)	201 ± 8	4.48 ± 0.27	4.84 ± 0.18
GO (0.5% PEI)	131 ± 4	2.71 ± 0.09	1.98 ± 0.07
GO (1% PEI)	253 ± 12	3.91 ± 0.44	5.51 ± 0.55
GO (2% PEI)	232 ± 13	3.04 ± 0.26	4.19 ± 0.56
GO (4% PEI)	122 ± 12	2.65 ± 0.28	1.84 ± 0.40
GO (0.5% $G4NH_2$)	209 ± 10	4.09 ± 0.23	4.47 ± 0.42
GO (1% $G4NH_2$)	253 ± 25	4.26 ± 0.43	5.75 ± 0.98
GO (2% $G4NH_2$)	238 ± 14	3.35 ± 0.28	4.55 ± 0.61
GO (4% $G4NH_2$)	212 ± 22	2.54 ± 0.40	3.02 ± 0.75
GO (5% PVP)	137 ± 9	1.50 ± 0.12	1.10 ± 0.16
GO (10% PVP)	190 ± 21	2.40 ± 0.22	2.39 ± 0.41
GO (15% PVP)	209 ± 17	2.63 ± 0.14	2.84 ± 0.28
GO (20% PVP)	196 ± 18	2.22 ± 0.21	2.35 ± 0.43
GO (5% PVA)	187 ± 26	2.84 ± 0.48	2.94 ± 0.79
GO (10% PVA)	236 ± 21	3.13 ± 0.55	3.95 ± 0.93
GO (15% PVA)	229 ± 15	2.46 ± 0.22	3.24 ± 0.52
GO (20% PVA)	190 ± 9	3.20 ± 0.34	3.13 ± 0.41
GO (5% PEO)	215 ± 15	4.05 ± 0.27	4.43 ± 0.52
GO (10% PEO)	236 ± 22	4.18 ± 0.30	5.02 ± 0.62
GO (15% PEO)	214 ± 6	4.04 ± 0.25	4.49 ± 0.31
GO (20% PEO)	182 ± 16	3.54 ± 0.51	3.54 ± 0.59
GO (5% CMC)	151 ± 12	1.74 ± 0.34	1.13 ± 0.27
GO (10% CMC)	194 ± 25	3.05 ± 0.50	2.97 ± 0.62
GO (15% CMC)	234 ± 20	3.70 ± 0.24	4.45 ± 0.58
GO (20% CMC)	184 ± 11	3.09 ± 0.12	3.06 ± 0.35
GO’ (evaporation)	141 ± 26	1.45 ± 0.26	1.17 ± 0.36
GO’ (1% Chitosan)	232 ± 20	3.81 ± 0.21	4.63 ± 0.45
GO’ (2% Chitosan)	279 ± 7	4.98 ± 0.23	6.32 ± 0.36
GO’ (4% Chitosan)	309 ± 21	5.22 ± 0.43	8.26 ± 0.68
GO’ (6% Chitosan)	218 ± 16	4.10 ± 0.47	5.01 ± 0.41
rGO’ (4% Chitosan)	424 ± 22	5.52 ± 0.39	8.98 ± 0.73

[a] Reported data on mechanical performances are the average of 5 independent samples.

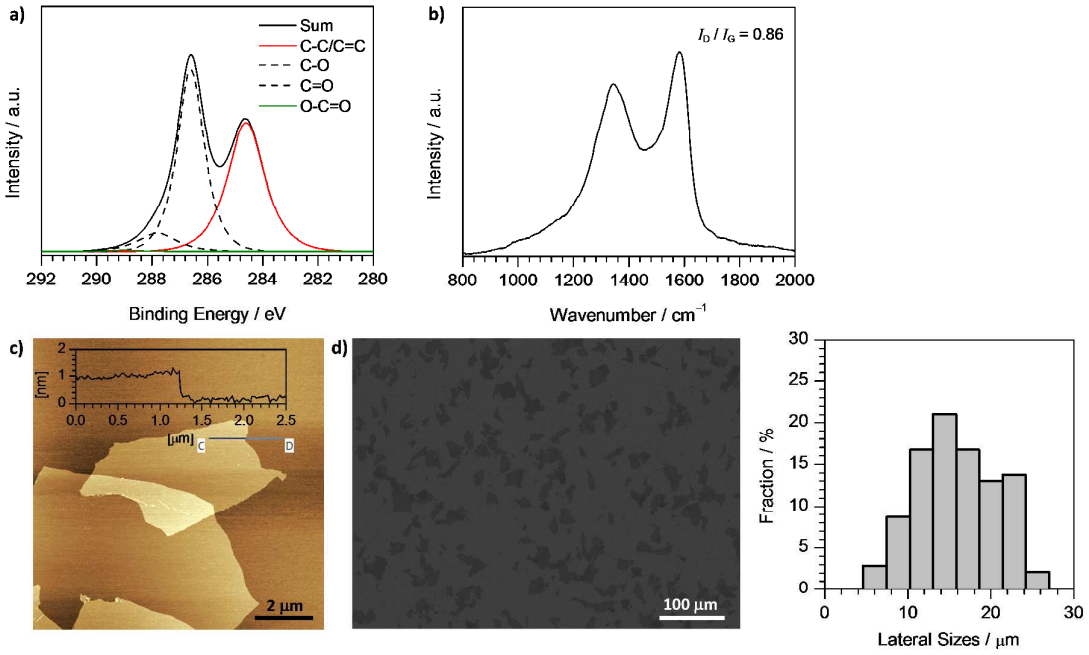

Figure S1. Structure characterization of GO sheets. (a) C1s XPS pattern and (b) Raman spectrum of GO sheets, (c) AFM image and cross section analysis of GO monolayer on mica. (d) SEM image of GO monolayer on silicon substrate and the histogram of GO size distribution based on SEM images.

High-solution XPS C1s scan indicated that carbon atoms within GO sheets form four types of covalent bonds: C–C/C=C (284.8 eV), C–O (287.0 eV), C=O (288.0 eV), and O–C=O (289.0 eV) (Figure S1a). The abundant oxygen-containing moieties attached on GO sheets enable GO hydrophilic and dispersible in water, forming a stable colloidal suspension. Raman spectrum of GO sheets is featured with broad and merged D and G bands at 1345 and 1583 cm^{-1}, respectively, with an intensity ratio (I_D/I_G) of 0.86, being characteristic of GO (Figure S1b). The thickness of GO sheets was measured to be 0.8 nm by the cross section analysis of AFM image (Figure S1c), being comparable to that of GO monolayer. The size distribution histogram based on a larger view of SEM image for GO sheets indicates that the lateral sizes of the GO sheets are widely distributed over a wide range with an average lateral size of 17 ± 5.0 µm (Figure S1d).

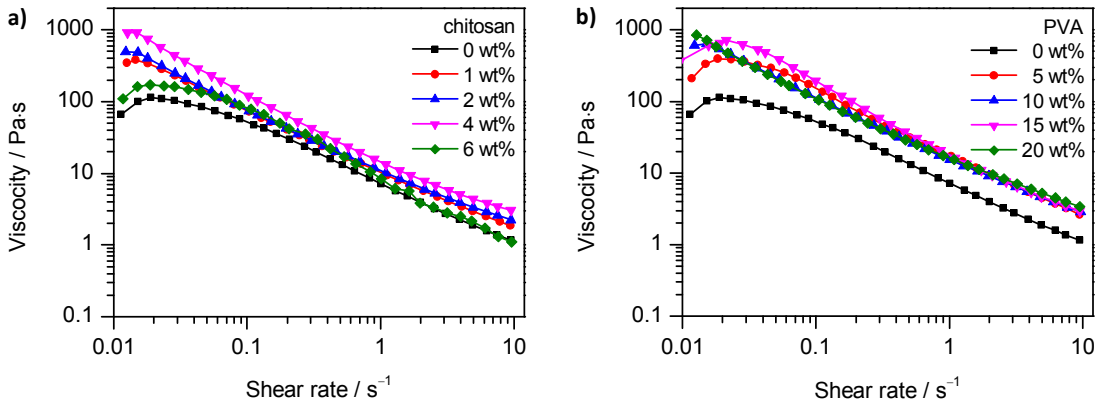

Figure S2. Viscosities at different shear rates of GO and GO/polymer mixtures containing different amounts of chitosan (a) and PVA (b).

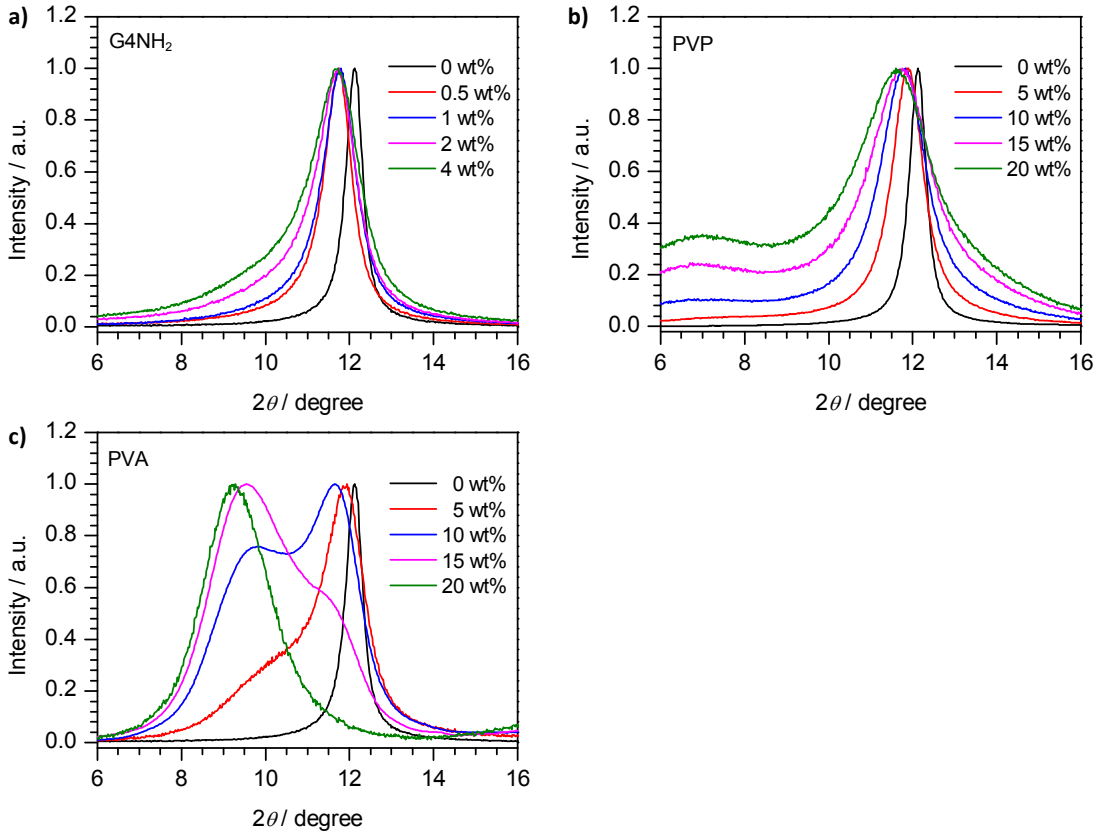

Figure S3. XRD patterns of the GO composite films containing different amounts of G4NH$_2$ (a), PVP (b), and PVA (c).

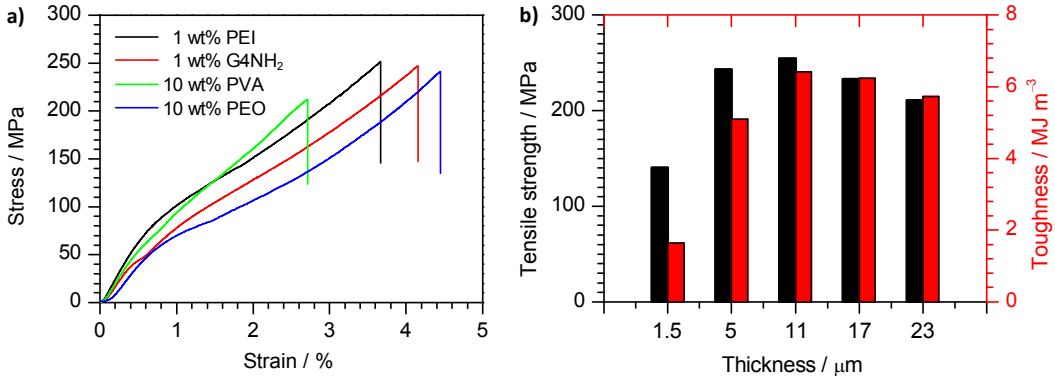

Figure S4. (a) Typical stress-strain curves of nacre-like GO films prepared by the GFT method. (b) Thickness-dependent mechanical performances of nacre-like GO films containing 4 wt% chitosan.

As shown in Figure S4b, the mechanical properties of the GO films are thickness-dependent, and both thinner and thicker films give poor performances. For thinner films, the detach-induced defects would be responsible for the attenuated mechanical properties. Whereas thickening the films will increase the number of defect sites within the films (based on the conventional fracture mechanics theory), and thus increase the possibility of crack initiation and alleviate the mechanical properties of the films (*Adv. Funct. Mater.* 2015, DOI: 10.1002/adfm.201500998).

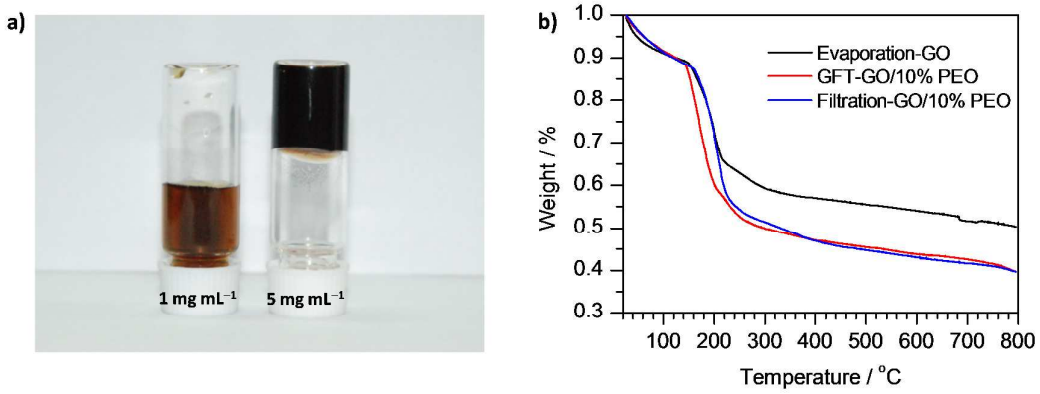

Figure S5. (a) Photographs of 1 and 5 mg mL^{-1} GO dispersions containing 10 wt% PEO. (b) TGA curves of GO and nacre-like GO films containing 10% PEO prepared by the methods as indicated.

As shown in Figure S5a, 1 mg mL^{-1} of GO dispersion containing 10 wt% PEO is existed in a sol phase, whereas 5 mg mL^{-1} of GO dispersion with 10 wt% PEO forms a hydrogel. TGA

measurements (Figure S5b) indicate that both GO/PEO films have similar components, and no obvious loss of PEO was observed, making it reliable to compare mechanical performances of nacre-like GO films prepared by these two approaches.

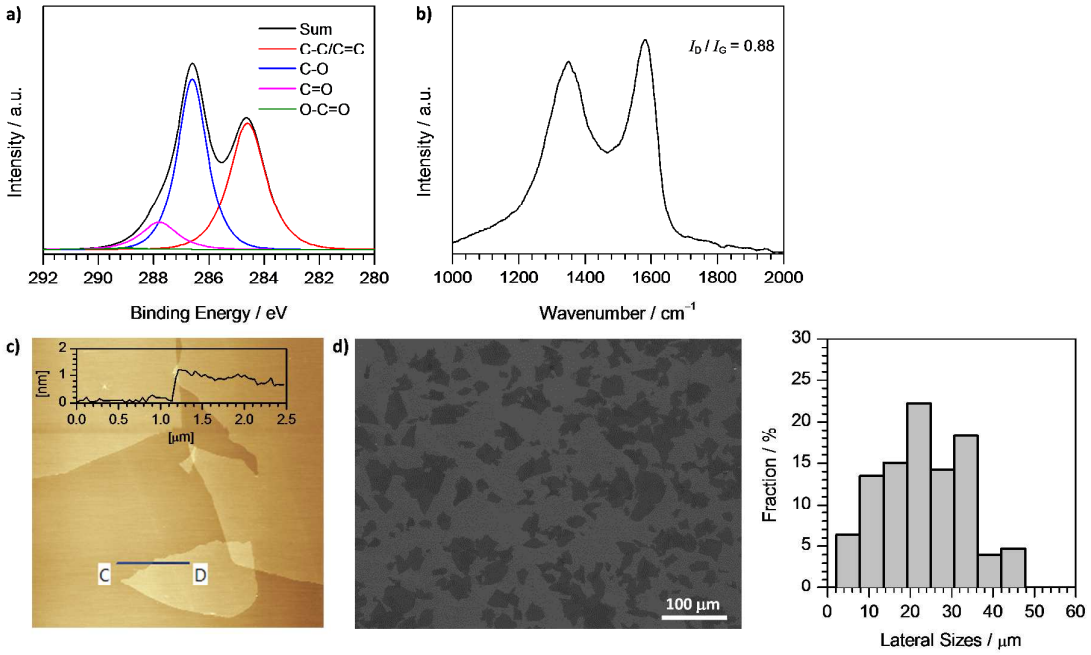

Figure S6. Structure characterization of GO' sheets. (a) C1s XPS pattern and (b) Raman spectrum of GO' sheets. (c) AFM image and cross section analysis of GO' monolayer on mica. (d) SEM image of GO' monolayer on silicon substrate and the histogram of GO' size distribution based on SEM images.

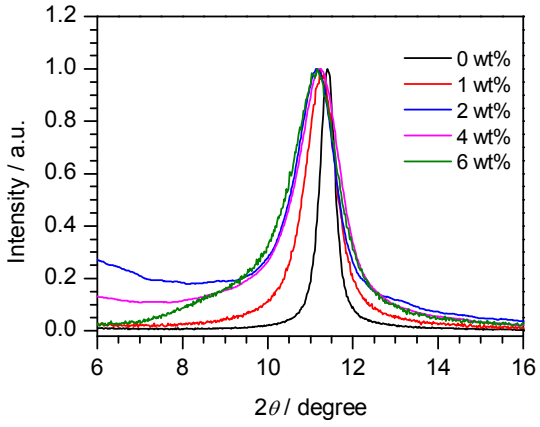

Figure S7. XRD patterns of the GO' composite films containing different amounts of chitosan.